Zarei et al., *BioImpacts.* 2025;15:30007
doi: 10.34172/bi.30007
https://bi.tbzmed.ac.ir/

Retinoic acid-releasing scaffold based on chitosan hydrogel and testis decellular plates

Hooman Zarei[1], Mansoureh Movahedin[1*], Fariba Ganji[2], Ali Ghiaseddin[3]

[1]Department of Anatomical Sciences, Faculty of Medical Sciences, Tarbiat Modares University, Tehran, Iran
[2]Biomedical Engineering Group, Faculty of Chemical Engineering, Tarbiat Modares University, Tehran, Iran
[3]Adjunct Research Associate Professor at Chemistry Department, Michigan State University, East Lansing, MI, USA

Article Info

Article Type:
Original Article

Article History:
Received: 25 Jul. 2023
Revised: 25 Nov. 2023
Accepted: 12 Dec. 2023
ePublished: 13 May 2024

Keywords:
Chitosan
Hydrogel
Releasing scaffold
Retinoic acid

Abstract

Introduction: The use of releasing scaffolds is promising for testes tissue engineering. Chitosan (CS) is a natural biopolymer extensively used as a delivery system. The decellularized testis provides a structure resembling natural extracellular matrix (ECM). All-trans retinoic acid (atRA) is an important factor for spermatogonia differentiation, meiosis completion, and mature sperm release. In this study, thermosensitive CS/βGP hydrogel was served as a novel atRA-releasing support for testis decellular plates (TDPs).

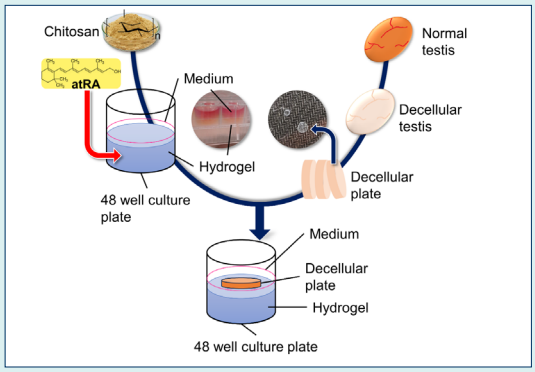

Methods: The CS/βGP hydrogel was evaluated for gelation time, morphology, wettability, cytocompatibility, and atRA-releasing behavior. Mouse testes were treated with 1% SDS and evaluated for decellularization efficacy through morphological assessments, DNA content assays, and DAPI staining. TDPs were obtained from the decellularized testes and placed on an atRA-releasing CS/βGP hydrogel support.

Results: The CS/βGP hydrogels were prepared with different formulations. It was found that increasing the βGP concentration significantly decreased the gelation time. The addition of atRA did not considerably affect the hydrophilicity of hydrogel. The in vitro release studies showed a sustained atRA release behavior, although an initial low burst release was recorded. Also, increasing the amount of atRA led to a decrease in the rate of drug release. The decellularization procedure successfully removed cells while preserving the ECM. The atRA-releasing CS-TDP scaffold was found to be non-toxic with good biocompatibility.

Conclusion: Results showed that the novel atRA-releasing CS-TDP scaffold can sustainably deliver atRA to the culture system and create a cytocompatible environment for testicular cells. Therefore, this scaffold may be useful in developing new tissue engineering approaches for various types of male infertility diseases.

Introduction

Releasing scaffold-based tissue engineering has emerged as a promising approach for regenerating damaged or lost tissues by providing a suitable environment for cell growth, differentiation, and proliferation. Simultaneously, it also delivers one or more specific molecules at a desired rate, facilitating functional tissue formation.[1,2] A key challenge in engineering releasing scaffolds is designing structures that mimic the target tissue's native extracellular matrix (ECM) while controlling molecule delivery.[3]

ECM scaffolds made of decellularized tissues are attractive for tissue engineering. The ECM is a complex network of proteins and carbohydrates that provides structural support, biochemical cues, and mechanical properties to cells and tissues. ECM scaffolds can be created by removing all cellular materials from natural tissues, maintaining their 3D structure and biological activity.[4] In this context, a decellularized testes matrix provides a natural ECM-like structure supporting cell adhesion, migration, and differentiation. Therefore, it

*Corresponding author: Mansoureh Movahedin, Email: mansoureh.movahedin@gmail.com

can be useful for in vitro spermatogenesis or testis-tissue engineering studies.[5] Baert et al introduced a method to prepare thin discs from a decellularized testes matrix to improve the accessibility of cells to the seminiferous tubules.[6] Later, Hashemi et al prepared thin plates from human decellularized testes and used them for in vitro spermatogenesis in a dynamic culture system.[7]

Chitosan (CS) is a natural biopolymer extensively used as a drug delivery system regarding its biocompatibility, biodegradability, antimicrobial, and mechanical properties.[8] Numerous CS formulations have been developed for the controlled release of both hydrophilic and hydrophobic molecules such as amoxicillin,[9] theophylline,[10] insulin,[11] fibroblast growth factor-2 (FGF-2),[12] dopamine,[13] venlafaxine,[14] and retinoic acid.[15] Recently, in-situ-forming thermosensitive hydrogels have garnered much attention for their potential applications in biomedicine, including drug delivery, tissue engineering, and enzyme or protein modifications.[2] Chenit et al introduced a remarkable injectable in situ gel-forming system based on a neutral solution of CS/beta-glycerophosphate disodium salt (βGP) combinations. This solution can remain in a liquid state at room temperature but transforms into a gel when heated to the body's physiological temperature (37 °C).[16]

All-trans retinoic acid (atRA) is a potent metabolite of vitamin A and a hydrophobic molecule that regulates various cellular processes. It is widely recognized that atRA plays a crucial role in spermatogenesis by aiding in the formation of the blood-testis barrier, promoting differentiation of spermatogonia, facilitating the release of mature sperm, and supporting the completion of meiosis.[17] However, the clinical use of atRA is limited due to its poor solubility, instability, and rapid metabolism.[18] To overcome these limitations, various drug delivery systems have been developed, including microspheres, liposomes, and hydrogels. In this respect, atRA-releasing CS systems were used in numerous studies. The carboxylate group in atRA has the potential to interact with the amino group in CS.[19] Mazini et al investigated the effect of atRA-loaded CS nanoparticles on spermatogenesis in mice subjected to scrotal hyperthermia. The findings reveal a notable enhancement in testicular health, testosterone levels, and sperm quality.[20] O'Leary et al designed a nanofibrous scaffold made of polycaprolactone and CS loaded with atRA, aiming for precise delivery in tracheal tissue regeneration.[21] Another research developed atRA-releasing nanoparticles using CS and tripolyphosphate lipid, intended for oral administration.[22]

The complexity of tissues and their functions requires more advanced and complex scaffolds that can mimic the native tissue's properties.[23] Therefore, the present research offers a novel scaffold comprising atRA-releasing CS/βGP hydrogel that serves as the support for the TDPs. One of the advantages of using thermosensitive CS is the possibility of adding the drug to the liquid state of the hydrogel at neutral pH, thereby preventing the degradation of sensitive drugs like atRA. Furthermore, using CS hydrogel could be a strategy to overcome the need for high drug doses for in vivo applications, as hydrophobic drugs such as atRA are quickly absorbed by the lymphatic system. Therefore, they require higher doses that can lead to side effects.[24]

Regarding the importance of atRA in spermatogenesis and limitations in ex vivo sperm production, such atRA-releasing CS-TDP scaffold may be promising for testis tissue engineering applications. This approach holds potential for male infertility therapies, particularly in prepubertal boys who need gonadotoxic treatments. Moreover, based on recent research, the incorporation of atRA into the scaffold can further enhance tissue regeneration by promoting cell proliferation and differentiation.[25]

This study aims to investigate the cytocompatibility of atRA-releasing CS-TDP scaffold and the impact of incorporating atRA on the characteristics of the CS/βGP hydrogel. Additionally, it is aimed to analyze the release patterns of atRA from the CS/βGP hydrogel.

Materials and Methods

Materials

Medium molecular weight CS (75-85% degree of deacetylation (DDA)), All-trans Retinoic acid (atRA), and 3-(4,5-dimethylthiazol-2-yl)-2,5-diphenyltetrazolium bromide (MTT) were obtained from Sigma Aldrich (St. Louis, MO). β-glycerophosphate disodium salt-pentahydrate (βGP, $C_3H_7Na_2O_6P.5H_2O$) and glacial acetic acid were purchased from Merck (Germany). Dimethyl sulphoxide (C_2H_6OS, DMSO) and Sodium lauryl sulphate ($C_{12}H_{25}NaO_4S$, SDS) were purchased from Carl Roth (Germany). Phosphate-Buffered Saline (PBS) tablets, MEM Alpha Medium (Minimum Essential Medium), fetal bovine serum (FBS), and antibiotics (penicillin, streptomycin) were purchased from Gibco (UK). Cryostat embedding medium (OCT) was obtained from Bio-Optica (Italy).

Preparation of decellular testes

The testes were isolated from male mice using standard dissection techniques. After sacrificing mice with chloroform, the scrotum was opened. Next, the testes were carefully removed and placed in a petri dish containing 1x PBS and 1% Pen/Strep. The isolated testes were then washed in 1x PBS to remove any blood and residual tissue debris. Afterward, the testes were transferred to a 50 mL conical tube containing 1% SDS solution and incubated in an orbital shaker (50 rpm) at room temperature for 24 h. The detergents were removed by washing the testes with 1x PBS for 24 h, and the PBS solution was changed every 6 h. Then, for disinfection, the decellular testes were

exposed to 4% ethanol with 0.1% peracetic acid for 2 h and washed again with 1x PBS for 3 h.[26]

Assessment of the decellularization procedure

Histological assessment

The decellularized testes were processed for histology using standard techniques. Briefly, the testes were fixed in 4% paraformaldehyde, dehydrated in a graded series of ethanol, and embedded in paraffin. Tissue sections (5 µm) were cut using a microtome and stained with H&E, Alcian Blue and Masson's Trichrome were used to analyze cellular and ECM components. Sections were evaluated and photographed with light microscopy (Zeiss AxioPhot).

Scanning electron microscopy

Scanning electron microscopy (SEM) was performed to assess the 3D structures of the decellularized and normal testes. The samples were fixed in 2.5% glutaraldehyde for 24 hours at 4 °C and then dehydrated in a graded series of alcohols. After embedding in paraffin, 5 µm sections were made, coated with gold, and imaged using an SEM device (TESCAN, Czechia).

DNA content assay

DNA was extracted from both normal and decellularized testes using the QIAamp DNA Mini Kit (Qiagen, Germany). The concentration of DNA was determined by measuring the absorbance at 260 nm using a NanoDrop 2000 C UV-Vis spectrophotometer (Thermo Scientific, Venlo, Netherlands). Each experiment was performed in quintuplicate to ensure accuracy and reproducibility.

DAPI staining

For nuclear staining, we used 4′,6-diamidino-2-phenylindole solution (DAPI, Sigma, USA). The samples were fixed in 4% paraformaldehyde and permeabilized with 0.1% Triton X-100 (Sigma, USA). Next, they were incubated with DAPI solution at a concentration of 1 µg/mL for 5-10 min in the dark. After staining, the samples were washed with PBS to remove any unbound DAPI. The stained samples were then visualized using a fluorescence microscope.

Preparation of testis decellular plates

Preparation of testis decellular plates (TDPs) from the decellularized testes were prepared according to the procedure described by Baert et al, with minor modifications.[6] Briefly, the decellularized testes were embedded in the OCT compound and allowed to freeze completely. The OCT-embedded testes were then cut into 250-350 µm thick sections using a cryostat microtome (Leica CM1850, Leica Biosystems, Germany). Finally, the TDPs were transferred into the dishes containing sterile PBS for washing the OCT compound remnants.

Preparation of atRA-loaded thermosensitive CS/βGP hydrogel

A clear solution was created by dissolving CS (200 mg) in 6 mL of aqueous glacial acetic acid (0.1 M) and sterilized by autoclaving at 120°C for 10 min. Varying amounts of βGP (400 mg and 700 mg) were dissolved in distilled water (2 mL) and filtered through a 0.22-µm syringe filter. The CS solution was cooled in an ice-water bath at 4 °C, followed by adding βGP solution dropwise while stirring. Afterward, a stock solution of atRA was prepared by dissolving 1.5 mg atRA in 1 mL PBS/DMSO (250 µL DMSO and 750 µL PBS). Amounts of 160 and 320 µL of atRA stock solution were diluted in distilled water to a final volume of 2 mL and were added slowly to the CS/βGP solution under continuous stirring. The final solution, with a total volume of 10 mL, was divided into 4 formulations (Table 1). Each formulation contained 2% (w/v) CS and either 4% or 7% (w/v) βGP, with or without atRA at concentrations of 80 or 160 µM. The concentration of DMSO was adjusted such that its final concentration in the culture condition did not exceed 0.5%. The solution was kept at 4 °C for further studies.

Evaluation of gelation time

The gelation time of the formulations was determined using the inverted tube test as outlined by Zhou et al.[27] For this purpose, 2 mL of hydrogel solutions were incubated in 5 mL vials with an inner diameter of 10 mm at 4 °C for 12 h to remove air bubbles. The vials were then transferred to a temperature-controlled bath at 34 °C, and the sol-gel transition was monitored by inverting the vials horizontally every minute. The gelation time was recorded when the gel ceased to flow. All measurements were performed in triplicate, and the data are expressed as means ± SD.

In vitro atRA stability

The in vitro stability of atRA was evaluated by preparing multiple microtubes containing a solution of a predetermined concentration of atRA in a mixture of PBS and DMSO. The microtubes were then incubated at 34 °C (since the spermatogenesis studies are done at this temperature) for up to 14 days. The absorbance

Table 1. Characteristics of CS/βGp Hydrogels with different formulations

Formulation	Chitosan (%w/v)	βGP (%w/v)	atRA Concentration (µM)	Gelation time[a] (min)
F1	2%	4%	0	20 ± 3 min
F2	2%	7%	0	9 ± 1 min
F3	2%	7%	80	7 ± 0.5 min
F4	2%	7%	160	6 ± 1.5 min

[a] All measurements were performed in triplicate; data are reported as means ± SD.

of the samples was measured at 350 nm using a UV spectrophotometer (Cary WinUV, Varian, Inc., Palo Alto, CA) at specific time points, and the decrease in absorbance over time was analyzed.[28] Each measurement was performed in triplicate, and the data were reported as means ± SD.

In vitro atRA release study

The atRA release profile was studied using formulations of CS (2% w/v) and βGp (7% w/v), containing atRA at concentrations of 80 and 160 µM (F3 and F4). The release test was conducted by adding 0.5 mL of the hydrogels into 2 mL microtubes. Once the gels had formed, 1 mL of phosphate buffer with a pH of 7.4 was added to each tube and incubated at 34°C. At specific time intervals (0, 5, 10, 24, 48, 120, and 168 h), 0.5 mL of phosphate buffer was collected and replaced with 0.5 mL of fresh buffer. After filtering the buffer, the amount of atRA release from scaffolds was determined using a UV spectrophotometer (Cary WinUV, Varian, Inc., Palo Alto, CA) at 350 nm. The absorption was compared with a calibration curve. Finally, the atRA release percentage was calculated according to the following formula[29]:

$$\text{Cumulative release \%} = \frac{\text{volume of sample withdrawn}}{\text{total volume}} \times C_{(n-1)} + C_n$$

which C_n = percentage atRA release at time (n); $C_{(n-1)}$ = percentage atRA release at time (n-1); Each determination was performed in triplicate.

Morphological evaluation of hydrogels by SEM

For the morphological evaluation of the hydrogels, samples with and without atRA (F2 and F4) were lyophilized for 24 h using a freeze-drier (Alpha 2-4 LDplus, Martin Christ, Germany) and then sectioned, gold coated, and scanned using SEM (TESCAN, Czechia). The resulting images were analyzed to determine the porosity and morphology of the hydrogels.

Wettability evaluation of hydrogels by WCA

The hydrogels' water contact angle (WCA) with and without atRA was measured using a Jikan CAG-20 device (Iran). To this end, the samples were placed on a slide, and a droplet of distilled water (10 µL) was gently placed onto the hydrogel surface using a microsyringe. The contact angle was measured immediately with a high-speed camera and analyzed. The measurements were repeated three times for each sample.

The cytocompatibility of atRA-releasing CS-TDP

To prepare the CS-TDP scaffold, the cryosectioned TDPs were placed and allowed to adhere to the atRA-releasing CS/βGP hydrogel support in a 96-well plate. MTT assay was used to assess the impact of atRA-releasing CS-TDP scaffold on mouse testicular cells in terms of viability, proliferation, and toxicity. To carry out the assay, the testicular cells were isolated from 6-day-old mice, seeded at a density of 2×10^4 in 96-well plates, and co-cultured with or without atRA-releasing CS-TDP scaffold. Following 24-, 48- and 72-hour incubation periods, the supernatant was removed, and the cells were treated with 0.5 mg/mL of MTT (Roth-Germany Carl) and incubated for four hours. The metabolized MTT (formazan) was then extracted by adding DMSO, followed by a 20-min incubation period. Lastly, the relative absorption of the eluted formazan was measured at 570 nm using a spectrophotometer.

Results and Discussion

Characterization of testicular decellular plates

Macroscopically, the color change from opaque to translucent white in the decellularized testes reflects successful cell removal. Histological evaluation through H&E, Trichrome Massone, and Alcian blue staining showed the effective removal of cellular materials, while ECM materials (i.e., collagen fibers and glycosaminoglycans) were retained (Fig. 1).

SEM images confirmed that the 3D structure of the seminiferous tubules was also preserved despite the removal of cellular parts (Figs. 2A-2D).

Further evaluation using DNA content assay and DAPI staining demonstrated an approximately 97.5% rate of DNA elimination and no detectable nuclei in the decellularized tissues (Fig. 3).

Researchers have previously prepared decellularized ECM from testes using various methods. Topraggaleh et al[30] and Majidi et al[31] used a mix of SDS and Triton X-100 over different time periods. Also, Baert et al found that using only 1% SDS resulted in efficient cell removal and improved ECM preservation.[5] Additionally, Hashemi et al suggested using SDS alone for decellularizing testes.[7] In conclusion, our findings suggest that decellularization efficiently removes cells while preserving the ECM.

Baert et al prepared thin discs from the decellularized testicular matrix to improve access to the acellular interstitial space and seminiferous tubules.[6] In the present study, we sterilized 250-350-µm thick slices of decellularized testes and placed them on top of the CS hydrogel. The resulting atRA-releasing CS-TDP scaffold was used for subsequent culture, as shown in Figs. 2E and 2F.

Characterization of atRA-releasing CS/βGP hydrogel

We prepared the CS/βGP hydrogels with different formulations (Table 1). The acidic CS solutions were neutralized by adding βGP salt dropwise without immediate gel formation. CS is a type of biopolymer carrying a positive charge and is not generally soluble in water. However, it can be dissolved in acidic aqueous solutions by protonating its amine groups. Once dissolved, CS can remain in the solution until the pH exceeds 6.2.[11] When CS solution is neutralized with a strong base up to pH 6.2, a hydrated gel-like precipitate is formed due to

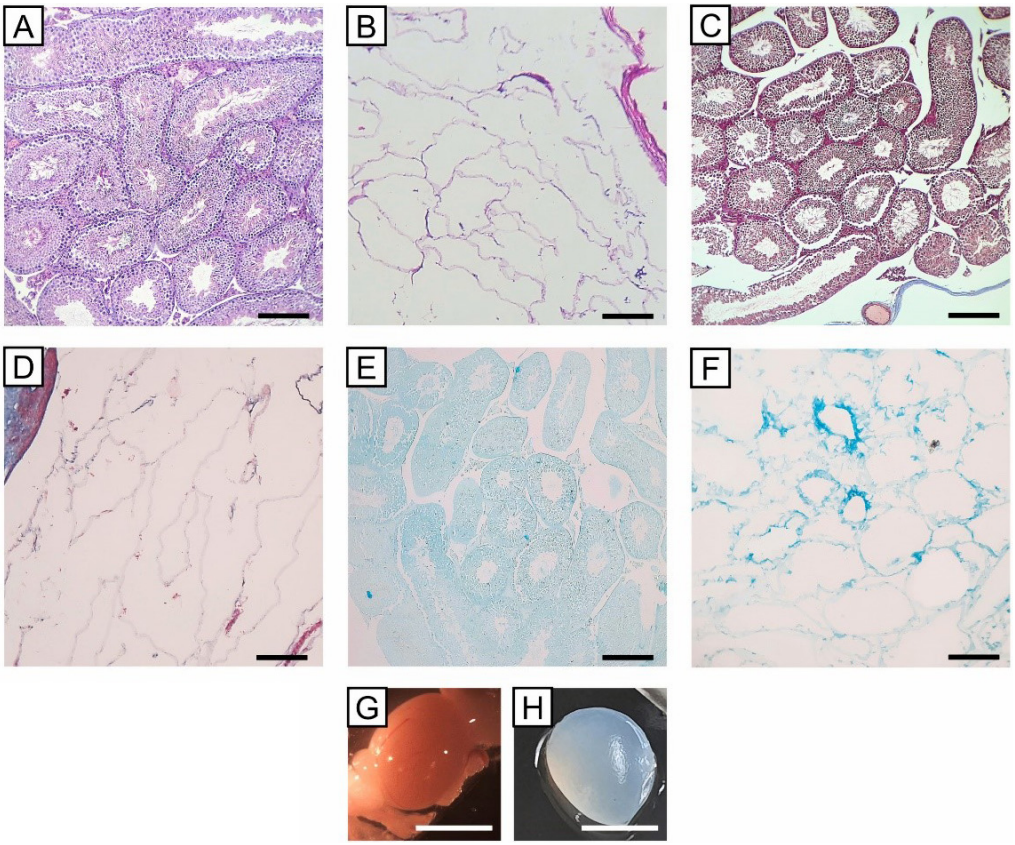

Fig. 1. Histologic and morphologic evaluation of decellularized mouse testis using SDS 1% for 24 h: A) H&E staining of normal testis showed seminiferous tubules; B) H&E staining of the decellular testis showed the elimination of the cells, and the remaining ECM; C) Masson's trichrome staining of the normal testis; D) Masson's trichrome staining of the decellular testis showed the retention of collagen fibers; E) Alcian blue staining of the normal testis; F) Alcian blue staining of the decellular testis showed retention of glycosaminoglycans (scale bars: 200 µm); G) Opaque color of normal testis; H) Translucent white color of the decellularized testis (scale bars: 5 mm)

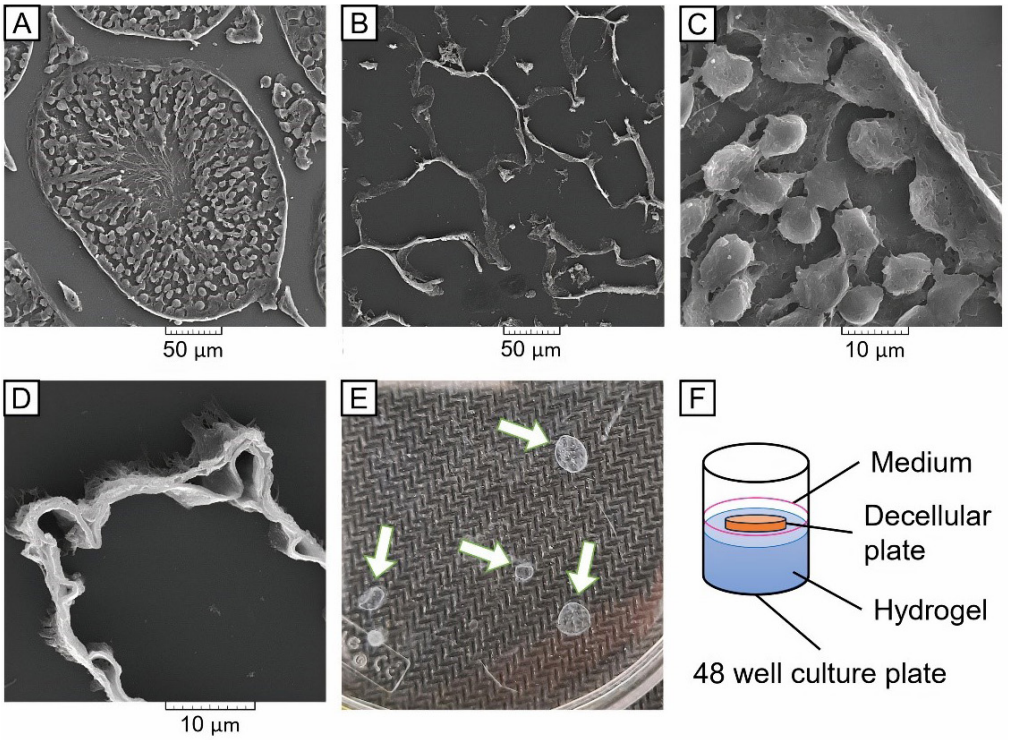

Fig. 2. SEM assessment of the Normal and Decellular testes plates: A) A seminiferous tubule of the normal testis with 500X magnification; B) Empty tubules of the decellular testis with 500X magnification showing the removal of cells; C) Seminiferous tubule-base of the normal testis with 3000X magnification; D) Seminiferous tubule wall of the decellular testis with 8000X magnification showed preservation of ECM; E) Morphology of TDPs with 250-350 µm thick; F) atRA-releasing CS-TDP scaffold used for subsequent culture.

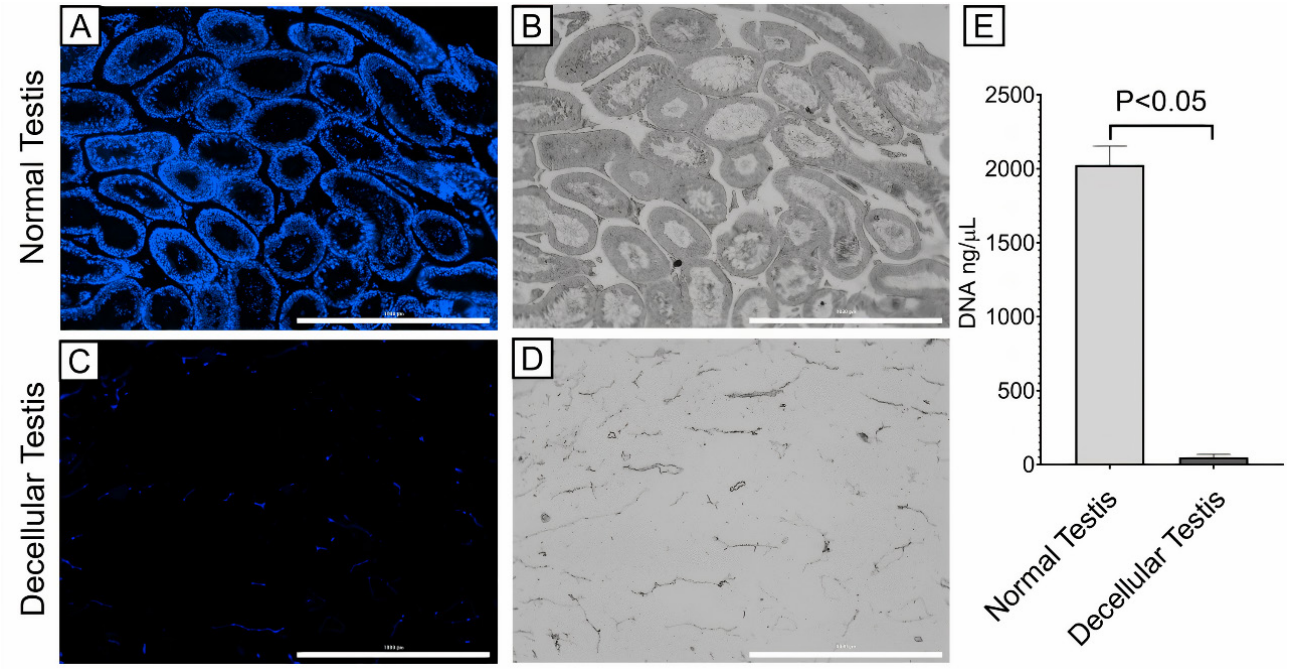

Fig. 3. Cell nuclei assessment by DAPI staining: A) DAPI staining showed the presence of cells in the normal testis; B) Phase contrast image of the normal testis; C) DAPI staining of the decellular testis showed no detectable nuclei, suggesting cell elimination; D) Phase contrast image of decellular testis (all scale bars: 1000 µm); E) DNA content assay showed 97.5% DNA elimination in the decellular testis group ($P<0.05$).

the elimination of repulsion between the positive charges of the CS amine groups. As a result, CS-CS hydrogen bonds form via various chemical groups, explained in previous studies.[32] Interestingly, an acidic CS solution can be neutralized up to a physiologic pH of 7.2 using βGP salt without immediate gel formation. βGP is a mono-headed salt with a counter-ionic polyol that acts as a base by neutralizing the acidic effect of the phosphate groups.

The gelation times of obtained CS/βGP hydrogels were investigated with the inverted test tube method at 34 °C. Although the acidic CS solution does not have thermosensitivity, subsequent heating of the CS/βGP solution leads to hydrogel formation. The sol/gel transition mechanism of the CS/βGP solution has been previously documented in studies by Cho et al and Li et al.[33,34] Basically, the mechanism involves the electrostatic attraction between the positively charged ammonium groups of CS and negatively charged phosphate moieties of βGP salt, which enables attractive hydrophobic and hydrogen bonding between CS chains.

The gelation time of CS solution with 4% βGP (F1) was obtained 20 min (± 3 min). It was found that increasing the βGP to 7% (F2) decreased gelation time up to 9 min (± 1 min). Therefore, it could be concluded that increasing the βGP concentration significantly decreased the gelation time ($P=0.019$). This result is consistent with the findings of Khodaverdi et al and Kempe's team.[8,35] Moreover, it was found that adding atRA decreased the gelation time, but not significantly (F3 and F4; $P=0.32$). These results indicate that increasing the βGP or atRA concentration could shorten the gelation time of CS hydrogels (Table 1). F2 was chosen for drug loading and further steps due to its shorter gelation time, which is beneficial for in vivo applications.

In vitro stability of atRA

UV-spectroscopy tracked the changes in atRA absorbance over 14 days in vitro. Fig. 4 illustrated that atRA maintained over 90% absorbance after 14 days at 34°C culture conditions, with no significant reduction ($P>0.05$).

In vitro release of atRA

previous studies demonstrated that the chemical reaction between atRA and CS was accomplished by coupling the carboxyl group of atRA with the amino groups of CS.[15] In this study, CS/βGp hydrogels were loaded with two different concentrations of atRA (F3 and F4), and its cumulative release behavior was investigated in vitro for each formulation. As shown in Fig. 5, increasing the amount of atRA led to a decrease in the rate of drug release, which is consistent with the observations made by Ghasemi et al [11] and Kim et al.[15]

The results suggest the slow release of the hydrophobic drug (like atRA as an insoluble compound in water) from CS/βGP hydrogel. Notably, atRA can form crystals when loaded at higher levels. Due to its hydrophobic nature, the crystallized drug can dissolve and/or release at a slower pace.[36] The early burst release of the atRA was not noteworthy, with only 33.3% and 9.3% of the atRA being released from samples F3 and F4, respectively, within a 24-h period. Following the initial burst release,

encapsulated atRA within the CS/βGp hydrogels was gradually released at a slower rate. As time progressed, the release rates of two samples decreased, which could be explained by the drug crystallization, declining amount of drug within the CS matrix, and a reduction in the concentration gradient of the drug.[37] This result is consistent with those of Hameed et al, who investigated cumulative release profile of ciprofloxacin from the CS hydrogel.[38]

Since spermatogenesis requires a low concentration of atRA,[39,40] formulation 4 was chosen for further steps and evaluations due to its desirable sustained release behavior and slower release rate.

Fig. 6 displays SEM images of a 6-µm thick section of F2 and F4 samples for evaluating the impact of atRA on the ultrastructure of the CS hydrogel. Both samples exhibit interconnecting highly porous structures, and the presence of atRA precipitation on the CS chains is clearly visible (Fig. 6B). Hydrophobic atRA seems crystalized on the hydrogel network. There are no obvious changes in the hydrogel structure and porosity. Consequently, it can be inferred that the addition of atRA does not significantly affect the porosity of the hydrogel.

The water contact angle was measured to determine the wettability of samples F2 and F4. Fig. 7 shows that the CS/βGP hydrogel has an average WCA of 24.5 ± 2.3°, while the atRA-releasing CS/βGP hydrogel has an average WCA of 31.3 ± 2.7°. The difference was significant ($P < 0.05$), but both are in the range of hydrophilicity. The findings suggest that adding a hydrophobic compound like atRA to CS hydrogel does not impact its hydrophilicity, which is crucial for cell-scaffold interactions, attachment, and proliferation.[41]

In vitro cytocompatibility of atRA-releasing CS-TDP

MTT assay was conducted to evaluate the biocompatibility of the atRA-releasing CS-TDP scaffold. MTT results represented that there was no significant difference between the viability of mouse testicular cells co-culturing with or without scaffolds after 24, 48, and 72

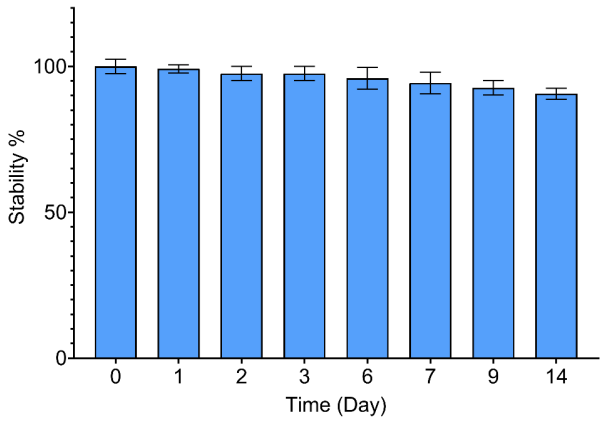

Fig. 4. The in vitro stability of atRA over 14 days was not significantly reduced, as measured by UV-Spectrophotometry ($P > 0.05$). Data are reported as means ± SD (n = 3).

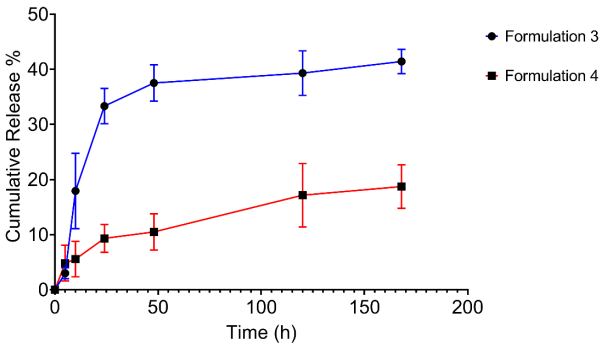

Fig. 5. The cumulative release profiles of two concentrations of atRA from CS/βGP hydrogels (F3 and F4); The initial release of atRA from F3 and F4 was not remarkable, with just 33.3% and 9.3% of atRA being released within the first 24 hours. After that, both formulations showed a more sustainable release behavior. The data are expressed as mean ± SD (n = 3).

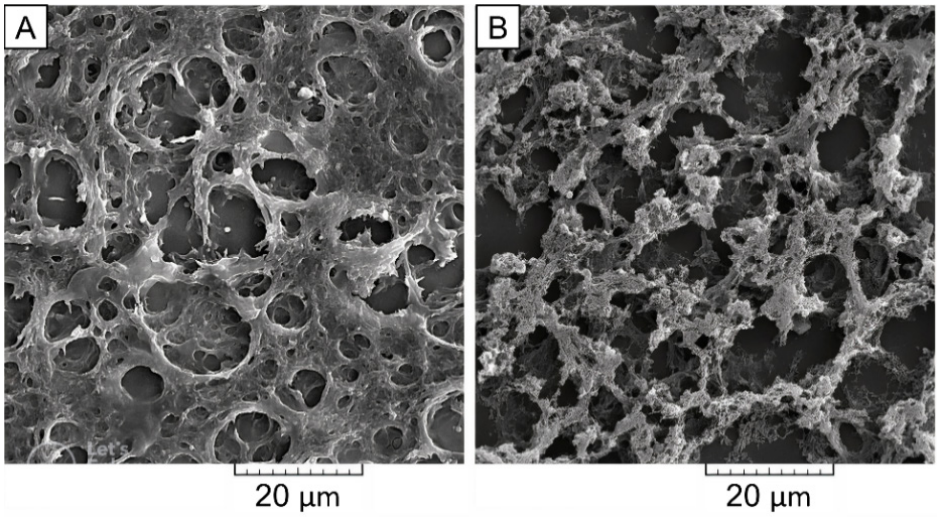

Fig. 6. SEM photographs of A) F2 and B) F4 samples; The atRA with its carboxylate group could interact with the amino group of CS and precipitate on the CS chains, which is visible in sample F4 (2000X magnification, scale bars: 20 µm).

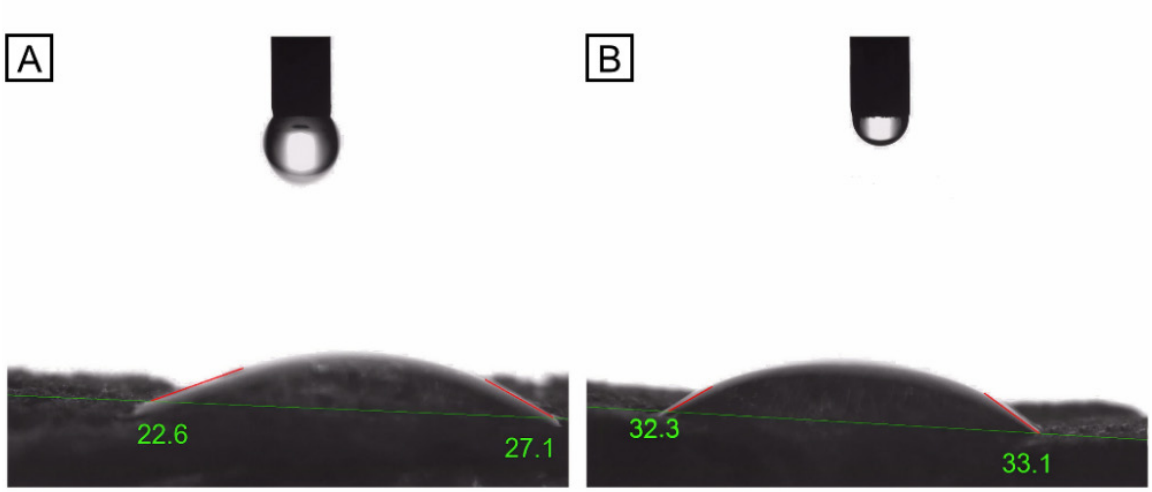

Fig. 7. WCA measurement for samples F2 and F4; A) CS/βGP hydrogel (F2) has 24.5±2.3 WCA°, indicating its hydrophilicity. B) atRA-releasing CS/βGP hydrogel (F4) has 31.3±2.7 WCA°, which is also in the range of hydrophilicity. Despite the significant difference, the addition of atRA did not affect the hydrogel's wettability. Data are reported as means±SD (n=3).

h of incubation ($P>0.05$) (Fig. 8). Even cell proliferation seems to increase gradually over time in scaffold groups (not significant), suggesting that the scaffolds are non-toxic and have good biocompatibility.

Scaffolds provide a 3D environment that allows cells to attach, migrate, and proliferate in a manner that more closely mimics their natural environment in vivo. This 3D structure provides a larger surface area for cell attachment and growth and more space for the cells to interact with each other and the surrounding extracellular matrix. As a result, cells in a scaffold-based 3D culture system can often grow and multiply more effectively than in a simple 2D culture.[42,43]

Conclusion

The results of this study demonstrate the potential of the decellularization protocol to eliminate the cellular materials from mouse testicular tissue while the resulting TDP maintained the native three-dimensional structure as well as important ECM components. The atRA-releasing CS-TDP scaffold can provide a cytocompatibe environment for mouse testicular cells. Also, it may enhance tissue regeneration by mimicking the native ECM and promoting the effects of atRA. The use of atRA-releasing CS/βGP hydrogel, compared to the manual addition of atRA, requires less drug and can deliver the drug to the system continuously with a low concentration. Also, atRA-releasing CS/βGP hydrogel could avoid the need for high doses of hydrophobic drugs for in vivo applications. These findings may have important implications for developing new therapies for various tissue injuries and diseases, including male infertility conditions.

Acknowledgements

The authors appreciate medical sciences faculty of Tarbiat Modares University for the pecuniary and instrumental support.

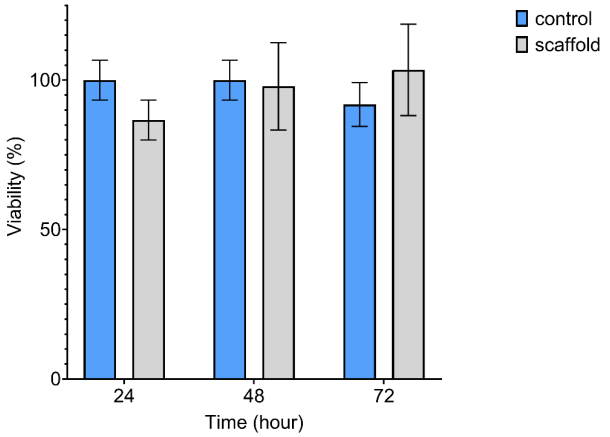

Fig. 8. Cytocompatibility assay of atRA-releasing CS-TDP scaffold by MTT test; The difference between the control and scaffold groups was not significant (P>0.05), suggesting that the scaffold is not toxic and is cytocompatible. Data are reported as means±SD (n=3).

Research Highlights

What is the current knowledge?

√ atRA is an important factor for spermatogenesis that should be considered in testes tissue engineering applications.

√ Decellularized tissues, which can be created by removing all cellular materials from natural tissues, are attractive for tissue engineering.

√ Chitosan (CS) is a natural biopolymer extensively used as a scaffold and a controlled delivery system.

What is new here?

√ The atRA-releasing CS/βGP hydrogel can be used as a sustainable drug delivery system.

√ The CS-TDP scaffold, prepared by using the atRA-releasing CS/βGP hydrogel as a support for TDP, could provide a cytocompatible environment for testicular cells without toxicity.

Authors' Contribution

Conceptualization: Mansoureh Movahedin, Fariba Ganji.
Data curation: Hooman Zarei, Fariba Ganji, Mansoureh Movahedin.
Investigation: Hooman Zarei.
Methodology: Ali Ghiaseddin, Fariba Ganji.
Resources: Mansoureh Movahedin, Fariba Ganji.
Supervision: Mansoureh Movahedin.
Validation: Fariba Ganji, Ali Ghiaseddin.
Writing-original draft: Hooman Zarei, Fariba Ganji.
Writing-review and editing: Hooman Zarei, Fariba Ganji, Mansoureh Movahedin.

Competing Interests

The authors declare no conflict of interests.

Ethical Statement

All animal procedures, experimental protocols, and methods were approved by the Ethics Committee of Tarbiat Modares University, Tehran, Iran (IR.MODARES.REC.1400.168).

Funding

This study was supported by the "Faculty of Medical Sciences at Tarbiat Modares University" and the "Iran's council for Development of Regenerative Medicine and Stem Cell Technologies".

References

1. Ma PX. Biomimetic materials for tissue engineering. *Adv Drug Deliv Rev* **2008**; 60: 184-98. https://doi.org/10.1016/j.addr.2007.08.041
2. Shoukat H, Buksh K, Noreen S, Pervaiz F, Maqbool I. Hydrogels as potential drug-delivery systems: network design and applications. *Ther Deliv* **2021**; 12: 375-396. https://doi.org/10.4155/tde-2020-0114
3. Aguilar LMC, Silva SM, Moulton SE. Growth factor delivery: Defining the next generation platforms for tissue engineering. *J Control Release* **2019**; 306: 40-58. https://doi.org/10.1016/j.jconrel.2019.05.028
4. Akbarzadeh A, Kianmanesh M, Fendereski K, Ebadi M, Daryabari SS, Masoomi A, *et al.* Decellularised whole ovine testis as a potential bio-scaffold for tissue engineering. *Reprod Fertil Dev* **2019**; 31: 1665-73. https://doi.org/10.1071/RD19070
5. Baert Y, Stukenborg J-B, Landreh M, De Kock J, Jörnvall H, Söder O, *et al.* Derivation and characterization of a cytocompatible scaffold from human testis. *Hum Reprod* **2015**; 30: 256-67. https://doi.org/10.1093/humrep/deu330
6. Baert Y, Goossens E. Preparation of scaffolds from decellularized testicular matrix. Decellularized Scaffolds and Organogenesis: Methods and Protocols. *Humana Press* **2018**; 121-7. https://doi.org/10.1007/7651_2017_29
7. Hashemi E, Movahedin M, Ghiaseddin A, Aghamir SMK. Dynamic Culture System Supports Mouse Spermatogenesis in Cell Culture Medium. *Pathobiol Res* **2022**; 25: 66-78.
8. Khodaverdi E, Tafaghodi M, Ganji F, Abnoos K, Naghizadeh H. In vitro insulin release from thermosensitive chitosan hydrogel. *AAPS PharmSciTech* **2012**; 13: 460-6. https://doi.org/10.1208/s12249-012-9764-9
9. Risbud MV, Hardikar AA, Bhat SV, Bhonde RR. pH-sensitive freeze-dried chitosan–polyvinyl pyrrolidone hydrogels as controlled release system for antibiotic delivery. *J Control Release* **2000**; 68: 23-30. https://doi.org/10.1016/S0168-3659(00)00208-X
10. Samanta HS, Ray SK. Controlled release of tinidazole and theophylline from chitosan based composite hydrogels. *Carbohydr Polym* **2014**; 106: 109-20. https://doi.org/10.1016/j.carbpol.2014.01.097
11. Ghasemi Tahrir F, Ganji F, Mani AR, Khodaverdi E. In vitro and in vivo evaluation of thermosensitive chitosan hydrogel for sustained release of insulin. *Drug Deliv* **2016**; 23: 1028-36. https://doi.org/10.4155/tde-2020-0114
12. Obara K, Ishihara M, Ishizuka T, Fujita M, Ozeki Y, Maehara T, *et al.* Photocrosslinkable chitosan hydrogel containing fibroblast growth factor-2 stimulates wound healing in healing-impaired db/db mice. *Biomaterials* **2003**; 24: 3437-44. https://doi.org/10.1016/S0142-9612(03)00220-5
13. Ren Y, Zhao X, Liang X, Ma PX, Guo B. Injectable hydrogel based on quaternized chitosan, gelatin and dopamine as localized drug delivery system to treat Parkinson's disease. *Int J Biol Macromol* **2017**; 105: 1079-87. https://doi.org/10.1016/j.ijbiomac.2017.07.130
14. Peng Y, Li J, Li J, Fei Y, Dong J, Pan W. Optimization of thermosensitive chitosan hydrogels for the sustained delivery of venlafaxine hydrochloride. *Int J Pharm* **2013**; 441: 482-90. https://doi.org/10.1016/j.ijpharm.2012.11.005
15. Kim D-G, Choi C, Jeong Y-I, Jang M-K, Nah J-W, Kang S-K, *et al.* All-trans retinoic acid-associated low molecular weight water-soluble chitosan nanoparticles based on ion complex. *Macromol Res* **2006**; 14: 66-72. https://doi.org/10.1007/BF03219070
16. Chenite A, Buschmann M, Wang D, Chaput C, Kandani N. Rheological characterisation of thermogelling chitosan/glycerol-phosphate solutions. *Carbohydr Polym* **2001**; 46: 39-47. https://doi.org/10.1016/S0144-8617(00)00281-2
17. Schleif MC, Havel SL, Griswold MD. Function of Retinoic Acid in Development of Male and Female Gametes. *Nutrients* **2022**; 14: 1293. https://doi.org/10.3390/nu14061293
18. Zheng A, Xie F, Shi S, Liu S, Long J, Xu Y. Sustained drug release from liposomes for the remodeling of systemic immune homeostasis and the tumor microenvironment. *Front Immunol* **2022**; 13. https://doi.org/10.3389/fimmu.2022.829391
19. Lira A, Nanclares D, Neto A, Marchetti J. Drug–polymer interaction in the all-trans retinoic acid release from chitosan microparticles. *J Therm Anal Calorim* **2007**; 87: 899-903. https://doi.org/10.1007/s10973-006-7684-1
20. Mazini F, Abdollahifar M-A, Niknejad H, Manzari-Tavakoli A, Zhaleh M, Asadi-Golshan R, *et al.* Retinoic acid loaded with chitosan nanoparticles improves spermatogenesis in scrotal hyperthermia in mice. *Korean J Fertil Steril* **2023**; 0. https://doi.org/10.5653/cerm.2023.06149
21. O'Leary C, Soriano L, Fagan-Murphy A, Ivankovic I, Cavanagh B, O'Brien FJ, *et al.* The Fabrication and in vitro Evaluation of Retinoic Acid-Loaded Electrospun Composite Biomaterials for Tracheal Tissue Regeneration. *Front Bioeng Biotechnol* **2020**; 8: 190. https://doi.org/10.3389/fbioe.2020.00190
22. Asfour MH, Salama AAA, Mohsen AM. Fabrication of All-Trans Retinoic Acid loaded Chitosan/Tripolyphosphate Lipid Hybrid Nanoparticles as a Novel Oral Delivery Approach for Management of Diabetic Nephropathy in Rats. *J Pharm Sci* **2021**; 110: 3208-20. https://doi.org/10.1016/j.xphs.2021.05.007
23. Place ES, George JH, Williams CK, Stevens MM. Synthetic polymer scaffolds for tissue engineering. *Chem Soc Rev* **2009**; 38: 1139-51. https://doi.org/10.1039/B811392K
24. Peers S, Montembault A, Ladavière C. Chitosan hydrogels for sustained drug delivery. *J Control Release* **2020**; 326: 150-63. https://doi.org/10.1016/j.jconrel.2020.06.012
25. Hlavac N, Bousalis D, Pallack E, Li Y, Manousiouthakis E, Ahmad RN, *et al.* Injectable Neural Hydrogel as in vivo Therapeutic Delivery Vehicle. *Regen Eng Transl Med* **2023**; 9: 424-30. https://doi.org/10.1007/s40883-022-00292-9
26. Duisit J, Amiel H, Wüthrich T, Taddeo A, Dedriche A, Destoop V, *et al.* Perfusion-decellularization of human ear grafts enables ECM-based scaffolds for auricular vascularized composite tissue engineering. *Acta Biomater* **2018**; 73: 339-54. https://doi.org/10.1016/j.actbio.2018.04.009
27. Zhou HY, Zhang YP, Zhang WF, Chen XG. Biocompatibility and characteristics of injectable chitosan-based thermosensitive hydrogel for drug delivery. *Carbohydr Polym* **2011**; 83: 1643-51. https://doi.org/10.1016/j.carbpol.2010.10.022
28. Wang F, He S, Chen B. Retinoic acid-loaded alginate microspheres as a slow release drug delivery carrier for intravitreal treatment. *Biomed Pharmacother* **2018**; 97: 722-8. https://doi.org/10.1016/j.biopha.2017.10.109

29. Chandrasekaran AR, Jia CY, Theng CS, Muniandy T, Muralidharan S, Dhanaraj SA. Invitro studies and evaluation of metformin marketed tablets-Malaysia. *J Appl Pharm Sci* **2011**; 214-7.
30. Topraggaleh TR, Valojerdi MR, Montazeri L, Baharvand H. A testis-derived macroporous 3D scaffold as a platform for the generation of mouse testicular organoids. *Biomater Sci* **2019**; 7: 1422-36. https://doi.org/10.1039/C8BM01001C
31. Gharenaz NM, Movahedin M, Mazaheri Z. Comparison of two methods for prolong storage of decellularized mouse whole testis for tissue engineering application: An experimental study. *Int J Reprod Biomed* **2021**; 19: 321.
32. Casettari L, Vllasaliu D, Castagnino E, Stolnik S, Howdle S, Illum L. PEGylated chitosan derivatives: Synthesis, characterizations and pharmaceutical applications. *Prog Polym Sci* **2012**; 37: 659-85. https://doi.org/10.1016/j.progpolymsci.2011.10.001
33. Li X, Kong X, Wang X, Shi S, Guo G, Luo F, *et al.* Gel–sol–gel thermo-gelation behavior study of chitosan–inorganic phosphate solutions. *Eur J Pharm Biopharm* **2010**; 75: 388-92. https://doi.org/10.1016/j.ejpb.2010.04.015
34. Cho J, Heuzey M-C, Bégin A, Carreau PJ. Physical gelation of chitosan in the presence of β-glycerophosphate: the effect of temperature. *Biomacromolecules* **2005**; 6: 3267-75. https://doi.org/10.1021/bm050313s
35. Kempe S, Metz H, Bastrop M, Hvilsom A, Contri RV, Mäder K. Characterization of thermosensitive chitosan-based hydrogels by rheology and electron paramagnetic resonance spectroscopy. *Eur J Pharm Biopharm* **2008**; 68: 26-33. https://doi.org/10.1016/j.ejpb.2007.05.020
36. Nishiyama N, Kataoka K. Preparation and characterization of size-controlled polymeric micelle containing cis-dichlorodiammineplatinum (II) in the core. *J Control Release* **2001**; 74: 83-94. https://doi.org/10.1016/S0168-3659(01)00314-5
37. Lira AAM, Rossetti FC, Nanclares DMA, Neto AF, Bentley MVLB, Marchetti JM. Preparation and characterization of chitosan-treated alginate microparticles incorporating all-trans retinoic acid. *J Microencapsul* **2009**; 26: 243-50. https://doi.org/10.1080/02652040802305105
38. Hameed AR, Mzoughi Z, Dammak MI, Jabrail FH, Le Cerf D, Majdoub H. Extraction, characterization and controlled release application of pectin-like/chitosan hydrogels system loaded Ciprofloxacin. *Curr Drug Deliv* **2023**. https://doi.org/10.2174/1567201821666230901153513
39. Yi H, Xiao S, Zhang Y. Stage-specific approaches promote in vitro induction for spermatogenesis. *In Vitro Cell Dev Biol Anim* **2018**; 54: 217-30. https://doi.org/10.1007/s11626-017-0216-4
40. Perrard M-H, Sereni N, Schluth-Bolard C, Blondet A, d′Estaing SG, Plotton I, *et al.* Complete human and rat ex vivo spermatogenesis from fresh or frozen testicular tissue. *Biol Reprod* **2016**; 95: 89. https://doi.org/10.1095/biolreprod.116.142802
41. Ghasemi-Mobarakeh L, Prabhakaran MP, Morshed M, Nasr-Esfahani M-H, Ramakrishna S. Electrospun poly(ε-caprolactone)/gelatin nanofibrous scaffolds for nerve tissue engineering. *Biomaterials* **2008**; 29: 4532-9. https://doi.org/10.1016/j.biomaterials.2008.08.007
42. Temenoff JS, Mikos AG. Tissue engineering for regeneration of articular cartilage. *Biomaterials* **2000**; 21: 431-40. https://doi.org/10.1016/S0142-9612(99)00213-6
43. Madl CM, Heilshorn SC, Blau HM. Bioengineering strategies to accelerate stem cell therapeutics. *Nature* **2018**; 557: 335-42. https://doi.org/10.1038/s41586-018-0089-z